IOP Publishing Phys. Scr. 98 (2023) 085217 https://doi.org/10.1088/1402-4896/ace392

Physica Scripta

RECEIVED
24 February 2023

REVISED
26 June 2023

ACCEPTED FOR PUBLICATION
3 July 2023

PUBLISHED
12 July 2023

PAPER

Solitons in fourth-order Schrödinger equation with parity-time-symmetric extended Rosen-Morse potentials

Jia-Rui Zhang[1], **Fang-Yu Zhu**[1], **Wan-Peng Li**[2] **and Yu-Jia Shen**[1,*]

[1] College of Science, China Agricultural University, Beijing 100083, People's Republic of China
[2] College of Water Resources and Civil Engineering, China Agricultural University, Beijing 100083, People's Republic of China
[*] Author to whom any correspondence should be addressed.

E-mail: chivalrous2387@163.com

Keywords: generalized nonlinear Schrödinger equation, fourth-order dispersion, $\mathcal{PT}$-symmetric extended Rosen-Morse potentials, stable nonlinear modes

Abstract

We investigate the fourth-order nonlinear Schrödinger equation modulated by parity-time-symmetric extended Rosen-Morse potentials. Since the imaginary part of the potentials does not vanish asymptotically, any slight fluctuations in the field can eventually cause the nonlinear modes to become unstable. Here we obtain stable solitons by adding the constraints of coefficients, which make the imaginary part of the potentials component vanish asymptotically. Furthermore, we get other fundamental stable single-hump and double-hump solitons by numerical methods. Then we consider excitations of the soliton via adiabatical change of system parameters. The results we obtained in this work provide a way to search for stable localized modes in parity-time-symmetric extended Rosen-Morse potentials with fourth-order dispersion.

1. Introduction

With the development of modern science and technology, the nonlinear characteristics of systems are considered fundamental to the understanding of many natural phenomena in various fields, such as fluid mechanics and nonlinear optics [1–5]. The nonlinear Schrödinger (NLE) equation

$$i\frac{\partial\psi}{\partial z} + \frac{\partial^2\psi}{\partial x^2} + [V(x) + iW(x)]\psi + \sigma|\psi|^2\psi = 0, \tag{1}$$

is a vital implement to describe nonlinear problems in physical systems and has been widely used in the study of various nonlinear phenomena, such as nonlinear optics, fluid mechanics, Bose–Einstein condensates, quantum optics, plasmas physics, finance, etc [6–11].

In fiber optics, the fourth-order dispersion effect of the NLS equation cannot be neglected when the pulse width is less than 10fs [12]. When the frequency of the optical field is close to the resonant frequency of the optical fiber material, it is necessary to introduce higher-order nonlinearity because the low-order nonlinear effect is not sufficient to describe the physical mechanism of the system [13, 14]. In this paper, we investigate the fourth-order generalized Schrödinger equation with quintic nonlinearities.

In 1998, Bender *et al* found that the non-Hermitian Hamiltonians, $\mathcal{H} = -\partial_x^2 + U(x)$ with complex-valued potentials can also exhibit entirely real spectra, which extended the traditional quantum theory to complex phase space [15]. This conclusion requires that non-Hermitian Hamiltonians are parity-time- ($\mathcal{PT}$-) symmetric. That is, the potential function satisfies $U(x) = U^*(-x)$ [16–18]. In optics, we can get the stable propagation of signal when the propagation constant of the light is in real spectrum range, which requires the gain-and-loss distributions in the medium to be precisely balanced to ensure the relation $n(x) = n^*(-x)$ [18, 19]. The introduction of the $\mathcal{PT}$-symmetry concept into optical systems led to the discovery of many stable solitons [20–30], in which the $\mathcal{PT}$-symmetric potential is realized by the complex refractive index $n(x) = n_R(x) + in_I(x)$ [31–33].

Over the past few years, various $\mathcal{PT}$-symmetric potentials have been introduced into the NLS equation [34–43]. In particular, in NLS equations with complex $\mathcal{PT}$-symmetric Scarf-II potentials [44–47], periodic potentials [48, 49], Gaussian potentials [50, 51], harmonic potentials [52–54], δ-signum potentials [55, 56], the existence of different nonlinear local modes is analytically and numerically investigated.

As an important three parameter molecular potential field, the standard Rosen-Morse potential can effectively describe the vibration of diatomic molecules [57]. What is more, Absolute transmission of the nonlinear system can occur in the hyperbolic Rosen-Morse potential with suitable complexification [58–63]. However, there are fewer studies on nonlinear modes in complex $\mathcal{PT}$-symmetric Rosen-Morse potential wells [64–66]. The complex Rosen-Morse potential has the same real part and different imaginary part as the Scarf-II potential. Since the imaginary part tends to a finite value rather than vanish asymptotically, the gain/loss is still there in the system even though it is far from the location [67]. Therefore, any slight fluctuations in the field can eventually cause the nonlinear modes to become unstable [64]. But we can set the imaginary part gradually disappear to obtain stable nonlinear modes by constructing the extended Rosen-Morse potentials. In this case, the complex potential can also be seen reduced to a generalized version of the $\mathcal{PT}$-symmetric Scarf-II potential [68].

In this paper, we investigate the propagation of nonlinear modes in a single $\mathcal{PT}$-symmetric waveguide cell characterized by the fourth-order generalized Schrödinger equation with quintic nonlinearities and extended complex Rosen-Morse potentials. The present paper is built up as follows. In section 2, the linear stability of solitons and stability of nonlinear modes in the NLS equation are analyzed. By adjusting the parameters of the extended Rosen-Morse potentials, we can obtain stable propagation of nonlinear modes. In section 3, we get other fundamental stable single-hump and double-hump solitons by numerical methods. Then we consider excitations of the soliton via adiabatical change of system parameters. In section 4, the results will be summarized.

2. Localized modes in NLS equation with $\mathcal{PT}$-symmetric complex potentials

2.1. Mathematical model

Here, we investigate the propagation of optical wave in a medium with fourth-order dispersion and quintic nonlinearities effects, which can be governed by the following generalized NLS equation with $\mathcal{PT}$-symmetric potentials [69, 70]:

$$i\frac{\partial\psi}{\partial z} + \frac{\partial^2\psi}{\partial x^2} - \beta\frac{\partial^4\psi}{\partial x^4} + [V(x) + iW(x)]\psi + \sigma|\psi|^2\psi + \gamma|\psi|^4\psi = 0, \tag{2}$$

where x and z are the transverse coordinate and scaled propagation distance, respectively, and $\psi(x, z)$ corresponds to the slowly varying amplitude of the light field. β represents the effect of fourth-order dispersion, $V(x)$ describes the real refractive index profile, and $W(x)$ is a gain-or-loss distribution. The $\mathcal{PT}$-symmetric potentials $V(x) + iW(x)$ leads to the conditions $V(x) = V(-x)$ and $W(x) = -W(-x)$. In this case, σ and γ are the parameters of cubic and quintic nonlinearities, respectively, and positive ones represent self-focusing nonlinear media, while negative ones represent self-defocusing nonlinear media.

We concentrate on stationary solutions of equation (2) in the form

$$\psi(x, z) = \phi(x)e^{i\mu z}, \tag{3}$$

where μ is the real propagation constant. The complex solution $\phi(x)$ satisfies the following condition

$$\left[\frac{d^2}{dx^2} - \beta\frac{d^4}{dx^4} + V(x) + iW(x) + \sigma|\phi|^2 + \gamma|\phi|^4\right]\phi = \mu\phi, \tag{4}$$

which can be solved using numerical methods for the given potentials $V(x) + iW(x)$ and real propagation constant μ.

We initiate our analysis by introducing the following $\mathcal{PT}$-symmetric potentials

$$V(x) = V_0\,\mathrm{sech}^2(x) + V_1\,\mathrm{sech}^4(x), \tag{5a}$$

$$W(x) = W_0\tanh(x) + W_1\tanh^3(x), \tag{5b}$$

and the constants V_0, V_1, W_0, and W_1 represent the depths of the real and imaginary parts. For the case $V_1 = W_1 = 0$, equation (5) simplifies to the standard Rosen-Morse potentials. These two functions are bounded and $V(x) \to 0$ while $|W(x)| \to |W_0 + W_1|$ as $|x| \to \infty$. Moreover, the gain-and-loss distribution can always be balanced in equation (2) since $\int_{-\infty}^{+\infty} W(x)dx = 0$.

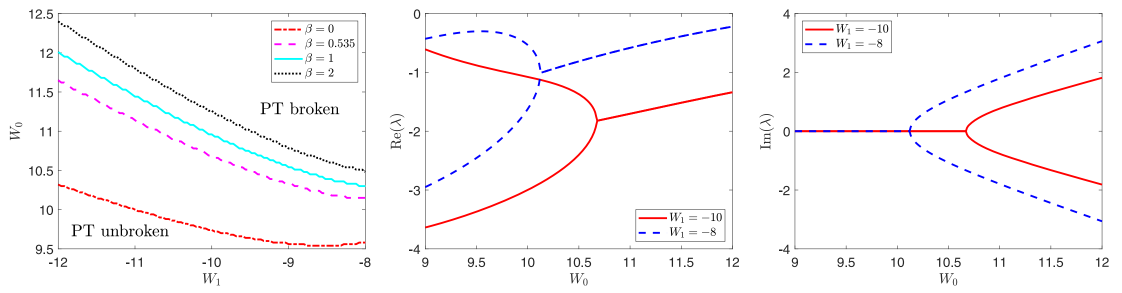

(a) (b) (c)

Figure 1. (a) The unbroken or broken $\mathcal{PT}$-symmetric phase generated by linear eigenvalue problem (7) with $\mathcal{PT}$-symmetric potentials (5). (b, c) Real and Imaginary part of the first two energy eigenvalues λ with $\beta = 0.535$. The parameters are $V_0 = 4.745$, $V_1 = 3$. The first two eigenvalues with the smallest real part correspond to the two lowest energy levels.

2.2. Linear eigenvalue problem

In the absence of the nonlinearity ($\sigma = \gamma = 0$), through the stationary transformation

$$\psi(x, z) = \phi(x)\mathrm{e}^{-i\lambda z}, \tag{6}$$

equation (4) can be transformed to the eigenvalue problem:

$$L\Phi(x) = \lambda\Phi(x), \tag{7a}$$

$$L = -\partial_x^2 + \beta\partial_x^4 - V(x) - iW(x), \tag{7b}$$

where λ and $\Phi(x)$ are the eigenvalue and the localized eigenfunction, respectively. We numerically solve the linear eigenvalue problem by the spectral method [71] and get the critical $\mathcal{PT}$-symmetry breaking lines on the (W_0, W_1) space, and the domains of unbroken/broken linear $\mathcal{PT}$-symmetric phases are above/below the $\mathcal{PT}$-symmetry breaking lines [see figure 1(a)]. It turns out that the unbroken domains become larger with the increase of β or the decrease of W_0 and W_1. For instance, we choose $W_1 = -10$ and -8 to illustrate the spontaneous $\mathcal{PT}$-symmetry breaking process, which stems from the collision of several lowest energy levels determined by discrete eigenvalue spectra [see figures 1(b) and 1(c)]. The first two eigenvalues with the smallest real part of the linear operator are the two lowest states corresponding to discrete spectra [15, 18, 72, 73]. The first two lowest energy levels begin to merge as W_0 increases, and the phase transition point is located at the boundary between the unbroken and the broken regions. This is due to the breakup of symmetry is associated with the increase of the imaginary part of the potential.

2.3. $\mathcal{PT}$ nonlinear mode and stability

In this section, we investigate the stationary solutions of equation (4) in the $\mathcal{PT}$-symmetric potentials (5). We have the analytical bright-soliton solution as [64]

$$\phi(x) = A\ \mathrm{sech}(x)\mathrm{e}^{ibx}, \tag{8}$$

where the amplitude soliton A, the phase wavenumber b, the propagation constant μ are given by:

$$A = \sqrt[4]{(24\beta - V_1)/\gamma}, \tag{9a}$$

$$b = \sqrt{(-2 + 20\beta + \sigma A^2 + V_0)/12\beta}, \tag{9b}$$

$$\mu = 1 - \beta b^4 + 6\beta b^2 - b^2 - \beta \tag{9c}$$

with $W_0 = 2b + 20\beta b + 4\beta b^3$, $W_1 = -24\beta b$, and the existing condition of the solution $(24\beta - V_1)\gamma > 0$ and $(-2 + 20\beta + \sigma A^2 + V_0)\beta > 0$ are required. Since $|W(x)| \to |W_0 + W_1|$ as $|x| \to \infty$, we can make $W_0 + W_1 = 0$ so that the imaginary part of the potentials component vanishes asymptotically with the increase of $|x|$ (i.e., $V_0 = -4 - 8\beta - \sigma A^2$).

For the nonlinear modes given in equation (8), the Poynting vector $S = \frac{i}{2}(\phi\phi_x^* - \phi^*\phi_x) = A^2 b\ \mathrm{sech}^2(x)$. Due to $A^2 b > 0$, S is positive everywhere, and the power flow in the $\mathcal{PT}$ cell is in one direction, i.e., from the gain domain towards the loss domain. The power of the solutions is $P = \int_{-\infty}^{\infty} |\phi(x)|^2 dx = 2A^2$. It remains positive and is conserved in the present condition of the solution.

Next, we investigate the linear stability of the nonlinear modes. We consider the perturbed solution $\psi(x, z)$, in the form

$$\psi(x, z) = \phi(x)\mathrm{e}^{i\mu z} + \epsilon[f(x)\mathrm{e}^{i\delta z} + g^*(x)\mathrm{e}^{-i\delta^* z}]\mathrm{e}^{i\mu z} \tag{10}$$

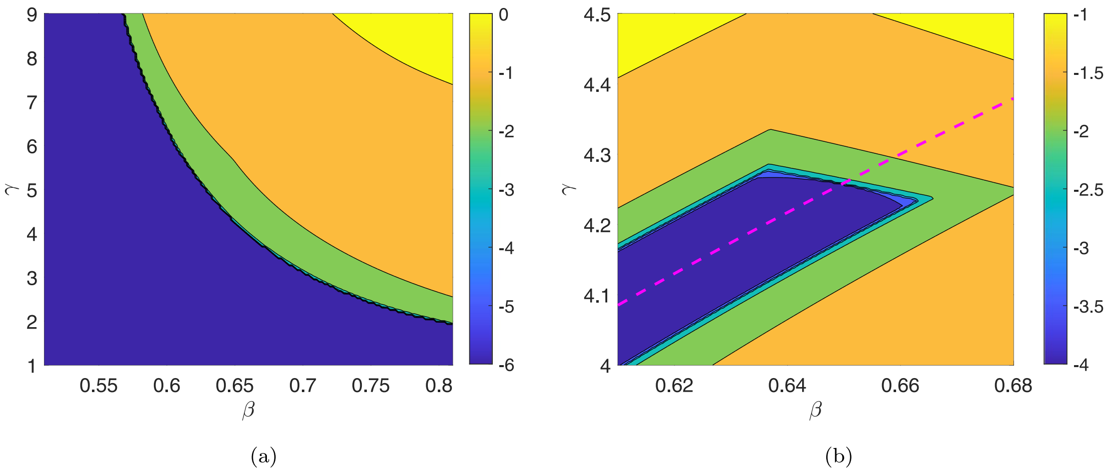

Figure 2. Maximal imaginary part of the linearization eigenvalue δ in the (β, γ)-space (common logarithmic scale), under the constraint of $\sigma = -10$, $V_1 = 3$ and (a) $V_0 = -4 - 8\beta - \sigma A^2$ and $b = \sqrt{(2\beta - 1)/2\beta}$; (b) $V_0 = 8$ and the parameters on the magenta dashed line satisfy $V_0 = -4 - 8\beta - \sigma A^2$.

where $\epsilon \ll 1$. $f(x)$ and $g(x)$ are the perturbation eigenfunctions of the linearized eigenvalue problem. By substituting equation (10) into equation (2) and linearizing with respect to ϵ, we obtain the following linear eigenvalue problem:

$$\begin{bmatrix} \hat{L}_1 & \hat{L}_2 \\ -\hat{L}_2^* & -\hat{L}_1^* \end{bmatrix} \begin{bmatrix} f(x) \\ g(x) \end{bmatrix} = \delta \begin{bmatrix} f(x) \\ g(x) \end{bmatrix}, \tag{11}$$

where

$$\hat{L}_1 = \partial_x^2 - \beta\partial_x^4 + V(x) + iW(x) + 2\sigma|\phi|^2 + 3\gamma|\phi|^4 - \mu, \tag{12a}$$

$$\hat{L}_2 = \sigma\phi^2 + 2\gamma|\phi|^2\phi^2. \tag{12b}$$

The imaginary part of δ measures the growth rate of the perturbation instability. If $|\mathrm{Im}(\delta)| > 0$, then the solution $\psi(x, z)$ will grow exponentially with z, and it is unstable; otherwise, the solution is stable. In our numerical simulation, we use the Fourier collocation method to discretize the associated differential operator as a matrix to solve the eigenvalue problem [74]. To further verify the stability of the solitons, we numerically investigate the stability by evolving them with 5% perturbations as the initial condition to simulate the random white noise (i.e., $\psi(x, 0) = \phi(x)(1 + \xi)$ and ξ represents 5% perturbations). In our numerical simulations, the second-order and fourth-order spatial differential is carried out by using Fourier spectral collocation method and the integration in time is carried out by using explicit fourth-order Runge-Kutta method [74].

As a result, under the constraint of $\sigma = -10$, $V_1 = 3$, we consider the cases of $V_0 = -4 - 8\beta - \sigma A^2$ (i.e., $W_0 + W_1 = 0$) and $V_0 = 8$, respectively. Then we get the stable (blue) and unstable (red) domains of nonlinear localized modes [see figures 2]. They are determined by the maximum absolute value of imaginary parts of the linearized eigenvalue δ in equation (11) in (β, γ) space. If $V_0 = -4 - 8\beta - \sigma A^2$ is satisfied, $b = \sqrt{(2\beta - 1)/2\beta}$ and some parameters make the nonlinear mode stable [see figure 2(a)]. We also can find that for a given V_0, when the parameters satisfy $-4 - 8\beta - \sigma A^2 = V_0$, the nonlinear mode tends to be stable [see figure 2(b)].

In particular, for the fixed parameters $\beta = 0.535$, $\sigma = -10$, $\gamma = 5.8$, $V_1 = 3$, figures 3(a)–(d) display the stable soliton for $V_0 = -4 - 8\beta - \sigma A^2$ while figures 3(e)–(h) display the unstable soliton for $V_0 = 8$; for the fixed parameters $\sigma = -10$, $\gamma = 4.68$, $V_0 = -4 - 8\beta - \sigma A^2$, $V_1 = 3$, figures 4(a)–(d) display the stable soliton for $\beta = 0.636$ while figures 4(e)–(h) display the unstable soliton for $\beta = 0.638$.

To sum up, when the imaginary part of the Rosen-Morse potentials well vanishes asymptotically, the soliton may be stable; otherwise, the soliton is unstable. Since the imaginary part does not vanishes asymptotically, the gain/loss remains in the system even far from the place of location. Therefore, any small fluctuations of the field are amplified/absorbed and lead to its instability eventually [64]. We can obtain stable solitons by the constraints of coefficients.

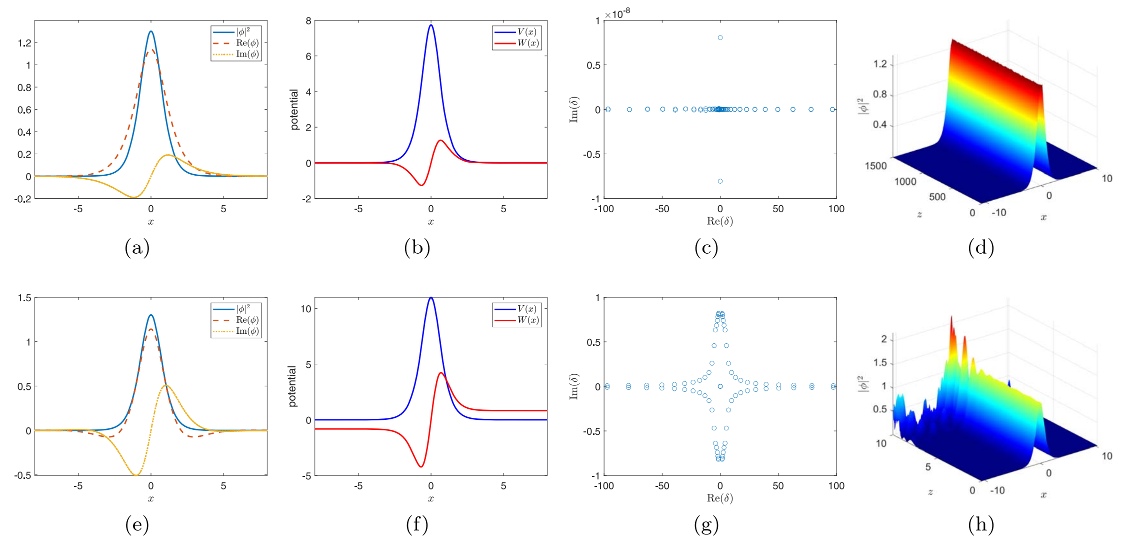

Figure 3. (a), (e) The soliton solutions. (b), (f) Real and imaginary parts of $\mathcal{PT}$-symmetric potentials. (c), (g) Linear stability eigenvalues. (d), (h) Stable or unstable propagations of nonlinear modes. The parameters are chosen as: $\beta = 0.535, \sigma = -10, \gamma = 5.8$, $V_1 = 3$, and (a)–(d) $V_0 = -4 - 8\beta - \sigma A^2$; (e–h) $V_0 = 8$.

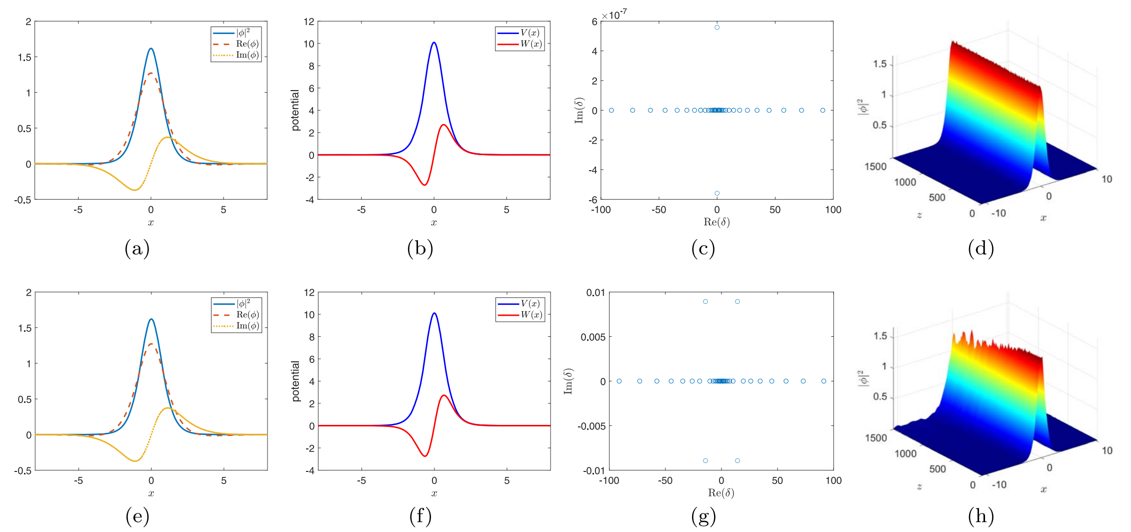

Figure 4. (a), (e) The soliton solutions. (b), (f) Real and imaginary parts of $\mathcal{PT}$-symmetric potentials. (c), (g) Linear stability eigenvalues. (d, h) Stable or unstable propagations of nonlinear modes. The parameters are chosen as: $\sigma = -10, \gamma = 4.68$, $V_0 = -4 - 8\beta - \sigma A^2, V_1 = 3$, and (a–d) $\beta = 0.636$; (e)–(h) $\beta = 0.638$.

3. Families and adiabatic excitations of nonlinear modes

3.1. Families of nonlinear modes

The above results have been obtained with the propagation constant $\mu = 1 - \beta b^4 + 6\beta b^2 - b^2 - \beta$, and it is difficult to find other solutions through analytical methods. However, we can get other fundamental solitons by numerical methods. When the parameters are chosen as $\beta = 0.535, \sigma = -10, \gamma = 5.8, V_0 = 4.745, V_1 = 3$, $W_0 = 3.284, W_1 = -3.284$, we carry out the modified squared-operator method [74] and get families of stable nonlinear modes, including single-hump and double-hump solitons (see figure 5(a)). For the same μ, we find another solution besides the analytic solution. We also use numerical evolution with 5% perturbations to verify the stability of the nonlinear modes. As shown in figures 6(a)–(d), we choose the solution (i.e., point B in figure 5(a)) with the same μ as the previous figure 3(a) (i.e., point A in figure 5(a)) and analyze its stability. From it, we can see that the solitons can propagate stably. Figures 6(e)–(h) show the double-hump soliton, corresponding to point C in figure 5(a), and we can see that the solution is in a critical steady state through the linear stability analysis and numerical evolution.

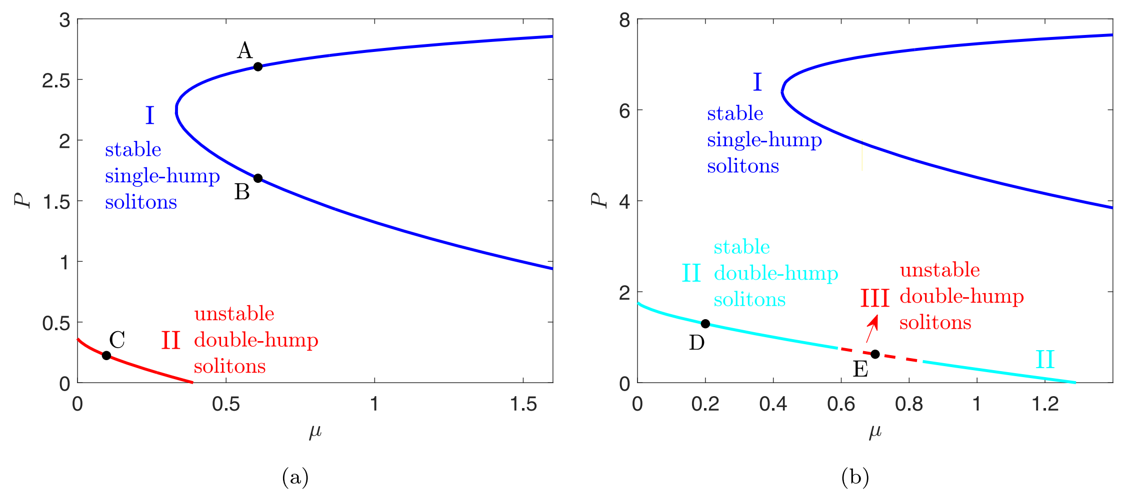

Figure 5. The power P of the numerical solitons versus the propagation constant μ. The parameters are chosen as: (a) $\beta = 0.535$, $\sigma = -10$, $\gamma = 5.8$, $V_0 = 4.745$, $V_1 = 3$, $W_0 = 3.284$, $W_1 = -3.284$; (b) $\beta = 0.6$, $\sigma = -5$, $\gamma = 1$, $V_0 = 9.503$, $V_1 = 1$, $W_0 = 5.879$, $W_1 = -5.879$. Points A and B correspond to the same μ. The soliton corresponding to point A is shown in figure 3(a).

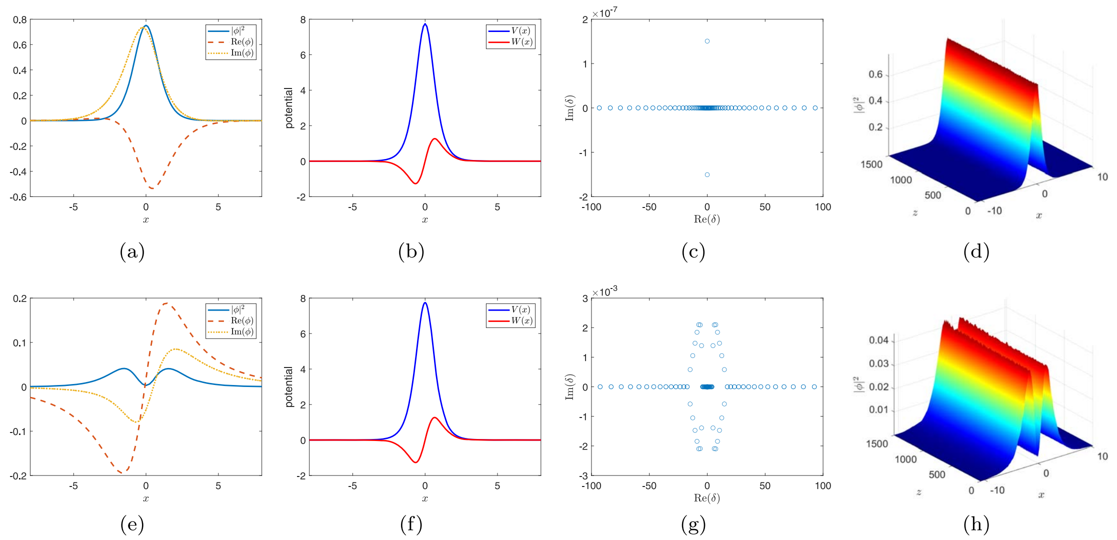

Figure 6. (a), (e) The soliton solutions. (b), (f) Real and imaginary parts of $\mathcal{PT}$-symmetric potentials. (c), (g) Linear stability eigenvalues. (d), (h) Stable or unstable propagations of nonlinear modes. The parameters are chosen as: $\beta = 0.535$, $\sigma = -10$, $\gamma = 5.8$, $V_0 = 4.745$, $V_1 = 3$, $W_0 = 3.284$, $W_1 = -3.284$. They correspond to points B and C in figure 5(a), respectively.

Next, we change the parameters to $\beta = 0.6$, $\sigma = -5$, $\gamma = 1$, $V_0 = 9.503$, $V_1 = 1$, $W_0 = 5.879$, $W_1 = -5.879$ and get other families of nonlinear modes [see figure 5(b)]. Figures 7(a)–(d) display the stable double-hump soliton with $\mu = 0.2$ while figures 7(e)–(h) display the unstable solution with $\mu = 0.7$.

3.2. Adiabatic excitations for the nonlinear modes

In this section, we consider excitations of the above-mentioned soliton in figure 3(a) via adiabatical change of system parameters. We change the parameters in equation (2) and $\mathcal{PT}$-symmetric potentials (5) as the functions of propagation distance z. To modulate the system parameters smoothly, we consider the following 'switch-on' function:

$$\epsilon(t) = \begin{cases} \epsilon^{(\text{ini})}, & t = 0, \\ \dfrac{\epsilon^{(\text{end})} - \epsilon^{(\text{ini})}}{2}\left[1 + \sin\left(\dfrac{\pi t}{500} - \dfrac{\pi}{2}\right)\right] + \epsilon^{(\text{ini})}, & 0 < t < 500, \\ \epsilon^{(\text{end})}, & 500 \leqslant t \leqslant 1500, \end{cases} \tag{13}$$

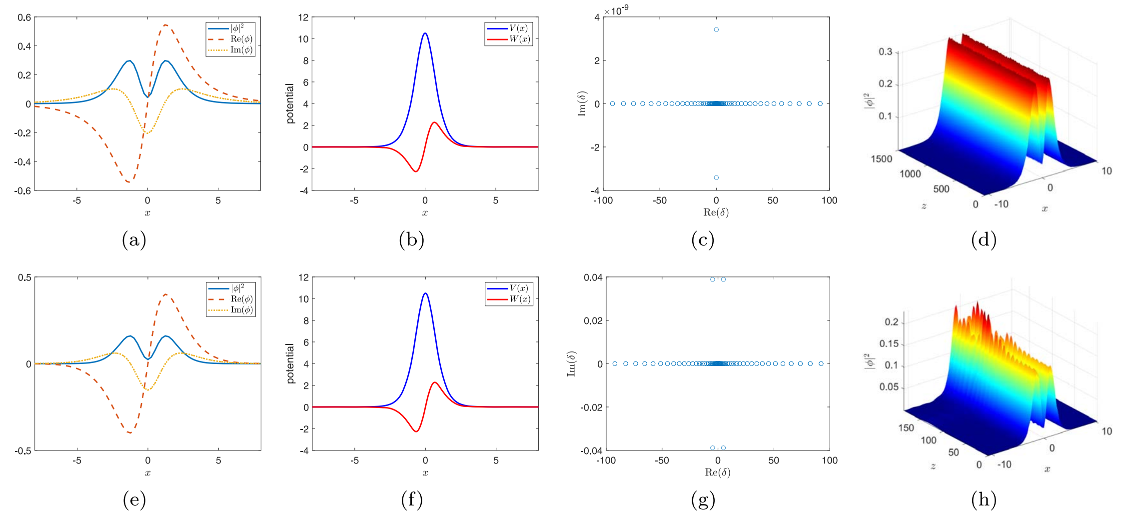

Figure 7. (a), (e) The soliton solutions. (b), (f) Real and imaginary parts of $\mathcal{PT}$-symmetric potentials. (c), (g) Linear stability eigenvalues. (d), (h) Stable or unstable propagations of nonlinear modes. The parameters are chosen as: $\beta = 0.6, \sigma = -5, \gamma = 1$, $V_0 = 9.503, V_1 = 1, W_0 = 5.879, W_1 = -5.879$. They correspond to points D and E in figure 5(b), respectively.

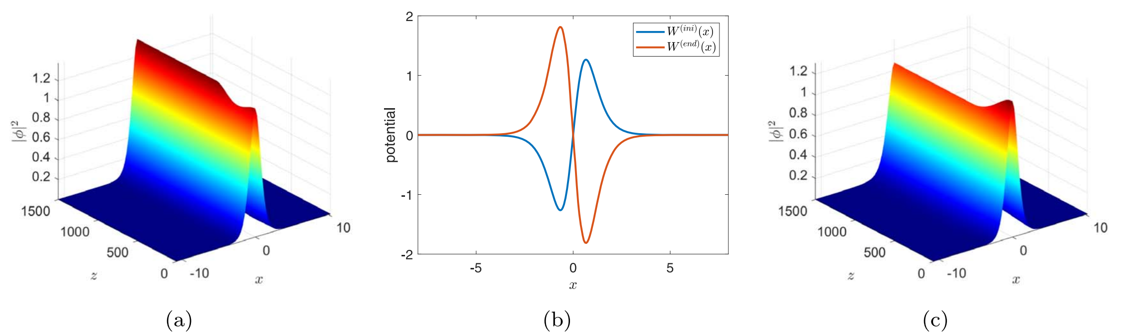

Figure 8. Adiabatic excitation of nonlinear mode and its evolution. The initial values of the excited state are the same as in figure 3(a): $\beta = 0.535, \sigma = -10, \gamma = 5.8, V_0 = 4.745, V_1 = 3, W_0 = 3.284, W_1 = -3.284$ and (a, b) $W_0^{(\mathrm{end})} = W_0^{(\mathrm{ini})} - 8$, $W_1^{(\mathrm{end})} = W_1^{(\mathrm{ini})} + 8$; (c) $\beta^{(\mathrm{end})} = \beta^{(\mathrm{ini})} + 0.5$.

where $\epsilon^{(\mathrm{ini})}$, $\epsilon^{(\mathrm{end})}$ respectively represent the real initial-state and final-state parameters. During the excitation stage ($0 < t < 500$), system parameters change slowly from $\epsilon^{(\mathrm{ini})}$ to $\epsilon^{(\mathrm{end})}$, and the initial state corresponding to $\epsilon^{(\mathrm{ini})}$ will be adiabatically driven to the new state corresponding to $\epsilon^{(\mathrm{end})}$; during the propagation stage ($500 \leqslant t \leqslant 1500$), system parameters are maintained at $\epsilon^{(\mathrm{end})}$, and the excited nonlinear mode will propagate in the final system [43, 75, 76]. To correspond to the content of the previous study, the initial values of the excited state are the same as in figure 3(a): $\beta = 0.535, \sigma = -10, \gamma = 5.8, V_0 = 4.745, V_1 = 3, W_0 = 3.284, W_1 = -3.284$.

We firstly change W_0 and W_1 by setting $W_0^{(\mathrm{ini})} = 3.284$, $W_0^{(\mathrm{end})} = -4.716$, $W_1^{(\mathrm{ini})} = -3.284$, $W_1^{(\mathrm{end})} = 4.716$, while keeping other parameters unchanged. Figure 8(a) show the stable excitation and evolution of the nonlinear mode. The initial and final states of the imaginary part of the complex potential well (i.e., gain-or-loss distribution) are shown in figure 8(b). We can find that the soliton can still propagate stably after the gain-or-loss distribution changes without other parameters being changed. Then we investigate the excitation of mode from a system of weak fourth-order dispersion to a strong one. In the parameters in the figure 2(a), as the effect of fourth-order dispersion increases, the soliton becomes unstable. In order to obtain stable soliton with strong fourth-order dispersion effects by adiabatic excitation, we change β by setting $\beta^{(\mathrm{ini})}=0.535$, $\beta^{(\mathrm{end})}=1.035$ while keeping other parameters unchanged. Finally we get stable soliton in figure 8(c).

4. Conclusion

In conclusion, we investigate the stability of nonlinear modes in the fourth-order nonlinear Schrödinger equation with quintic nonlinearities and $\mathcal{PT}$-symmetric extended Rosen-Morse potentials analytically and numerically. For the $\mathcal{PT}$-symmetric extended Rosen-Morse potentials, the parameter space can be divided into different domains corresponding to unbroken and broken $\mathcal{PT}$-symmetry. Since the imaginary part of the potentials does not vanish asymptotically, any slight fluctuations in the field are amplified/absorbed and can eventually cause the nonlinear modes to become unstable. Here we obtain stable solitons by adding the constraints of coefficients, which make the imaginary part of the potentials component vanish asymptotically. And we investigate the linear stability of the nonlinear modes and validate the results by evolving them with 5% perturbations as an initial condition. We also investigate the Poynting vector and the power of nonlinear modes, which are positive everywhere. And in the $\mathcal{PT}$ cell, the power flow is in one direction, i.e., from the gain domain toward the loss domain. Furthermore, we can get other fundamental stable single-hump and double-hump solitons by numerical methods. Finally, we consider excitations of the soliton via adiabatical change of system parameters.

The results we obtained in this work provide a way to search for the stable localized modes of the nonlinear Schrödinger equation with the $\mathcal{PT}$-symmetric extended Rosen-Morse potentials with fourth-order diffraction. These findings of nonlinear modes can be potentially applied to hydrodynamics, optics, and matter waves in Bose–Einstein condensates.

Acknowledgments

We express our sincere thanks to the editor, referees, and all the members of our discussion group for their valuable comments. This work was supported by the National Training Program of Innovation (Grant number 202 210 019 045). The funding body plays an important role in the design of the study, in analysis, calculation, and in writing of the manuscript.

Data availability statement

No new data were created or analysed in this study.

Declarations of interest

None.

ORCID iDs

Yu-Jia Shen https://orcid.org/0000-0003-1484-5584

References

[1] Haken H 1975 Generalized Ginzburg-Landau equations for phase transitionlike phenomena in lasers, nonlinear optics, hydrodynamics and chemical reactions *Z. Phys.* B **21** 105
[2] Musslimani Z H, Makris K G, El-Ganainy R and Christodoulides D N 2008 Optical solitons in $\mathcal{PT}$ periodic potentials *Phys. Rev. Lett.* **100** 030402
[3] Konotop V V, Yang J and Zezyulin D A 2016 Nonlinear waves in $\mathcal{PT}$-symmetric systems *Rev. Mod. Phys.* **88** 035002
[4] Kartashov Y V, Astrakharchik G E, Malomed B A and Torner L 2019 Frontiers in multidimensional self-trapping of nonlinear fields and matter *Nature Rev. Phys.* **1** 185–97
[5] Mihalache D 2015 Localized structures in optical and matterwave media: a selection of recent studies *Rom. Rep. Phys.* **67** 1383–400
[6] Ablowitz M J and Clarkson P A 1991 *Solitons, Nonlinear Evolution Equations and Inverse Scattering* (Cambridge: Cambridge University Press)
[7] Kivshar Y S and Agrawal G 2003 *Optical Solitons: from Fibers to Photonic Crystals* (San Diego: Academic)
[8] Pitaevskii L and Stringari S 2003 *Bose-Einstein Condensation* (Oxford: Oxford University Press)
[9] Kharif C, Pelinovsky E and Slunyaev A 2009 *Rogue Waves in the Ocean* (New York: Springer)
[10] Osborne A 2010 *Nonlinear Ocean Waves and the Inverse Scattering Transform* (New York: Elsevier)
[11] Yan Z 2010 Financial rogue waves *Commun. Theor. Phys.* **54** 947
[12] Haus H A and Wong W S 1995 *Solitons in Optical Communications* (Oxford: Oxford University Press)
[13] Agrawal G P 2005 *Nonlinear Fiber Optics* (New York: Academic)
[14] Maimistov A I and Basharov A M 1999 *Nonlinear Optical Waves* (Amsterdam: Kluwer Academic)
[15] Bender C M and Boettcher S 1998 Real spectra in non-hermitian hamiltonians having $\mathcal{PT}$ symmetry *Phys. Rev. Lett.* **80** 5243
[16] Bender C M, Brody D C and Jones H F 2003 Must a Hamiltonian be Hermitian? *Am. J. Phys.* **71** 1095–102
[17] Bender C M 2016 Rigorous backbone of $\mathcal{PT}$-symmetric quantum mechanics *J. Phys.* A **49** 401002
[18] Bender C M 2007 Making sense of non-Hermitian Hamiltonians *Rep. Prog. Phys.* **70** 947
[19] Yan Z, Wen Z and Hang C 2015 Spatial solitons and stability in self-focusing and defocusing Kerr nonlinear media with generalized parity-time-symmetric Scarff-II potentials *Phys. Rev.* E **92** 022913
[20] Driben R and Malomed B A 2011 Stability of solitons in parity-time-symmetric couplers *Opt. Lett.* **36** 4323–5
[21] Wang H and Wang J 2011 Defect solitons in parity-time periodic potentials *Opt. Express* **19** 4030–5

[22] He Y, Zhu X, Mihalache D, Liu J and Chen Z 2012 Lattices solitons in $\mathcal{PT}$-symmetric mixed linear-nonlinear optical lattices *Phys. Rev.* A **85** 013831
[23] Zezyulin D A, Kartashov Y V and Konotop V V 2011 Stability of solitons in $\mathcal{PT}$-symmetric nonlinear potentials *Europhys. Lett.* **96** 64003
[24] Zezyulin D A and Konotop V V 2012 Nonlinear modes in finite-dimensional $\mathcal{PT}$-symmetric systems *Phys. Rev. Lett.* **108** 213906
[25] Mayteevarunyoo T, Malomed B A and Reoksabutr A 2013 Solvable model for solitons pinned to a parity-time-symmetric dipole *Phys. Rev.* E **88** 022919
[26] Kartashov Y V, Malomed B A and Torner L 2014 Unbreakable $\mathcal{PT}$ symmetry of solitons supported by inhomogeneous defocusing nonlinearity *Opt. Lett.* **39** 5641–4
[27] Miri M-A, Aceves A B, Kottos T, Kovanis V and Christodoulides D N 2012 Bragg solitons in nonlinear $\mathcal{PT}$-symmetric periodic potentials *Phys. Rev.* A **86** 033801
[28] Karjanto N, Hanif W, Malomed B A and Susanto H 2015 Interactions of bright and dark solitons with localized $\mathcal{PT}$-symmetric potentials *Chaos* **25** 023112
[29] Malomed B A 2015 Nonlinear optics: symmetry breaking in laser cavities *Nat. Photonics* **9** 287
[30] Alexeeva N V, Barashenkov I V, Sukhorukov A A and Kivshar Y S 2012 Optical solitons in $\mathcal{PT}$-symmetric nonlinear couplers with gain and loss *Phys. Rev.* A **85** 063837
[31] Guo A, Salamo G J, Duchesne D, Morandotti R, Volatier-Ravat M, Aimez V, Siviloglou G A and Christodoulides D N 2009 Observation of $\mathcal{PT}$-symmetry breaking in complex optical potentials *Phys. Rev. Lett.* **103** 093902
[32] Bendix O, Fleischmann R, Kottos T and Shapiro B 2009 Exponentially fragile $\mathcal{PT}$ symmetry in lattices with localized eigenmodes *Phys. Rev. Lett.* **103** 030402
[33] Rüter C E, Makris K G, Ganainy R, Christodoulides D N, Segev M and Kip D 2010 Observation of parity-time symmetry in optics *Nat. Phys.* **6** 192–5
[34] Shi Z, Jiang X, Zhu X and Li H 2011 Bright spatial solitons in defocusing Kerr media with $\mathcal{PT}$-symmetric potentials *Phys. Rev.* A **84** 053855
[35] Nixon S, Ge L and Yang J 2012 Stability analysis for solitons in $\mathcal{PT}$-symmetric optical lattices *Phys. Rev.* A **85** 023822
[36] Hu S and Hu W 2012 Optical solitons in the parity-time-symmetric Bessel complex potential *J. Phys.* B **45** 225401
[37] Khare A, Al-Marzoug S M and Bahlouli H 2012 Solitons in $\mathcal{PT}$-symmetric potential with competing nonlinearity *Phys. Lett.* A **376** 2880
[38] Achilleos V, Kevrekidis P G, Frantzeskakis D J and Carretero-Gonzalez R 2012 Dark solitons and vortices in $\mathcal{PT}$-symmetric nonlinear media: from spontaneous symmetry breaking to nonlinear $\mathcal{PT}$ phase transitions *Phys. Rev.* A **86** 013808
[39] Lumer Y, Plotnik Y, Rechtsman M C and Segev M 2013 Nonlinearly Induced $\mathcal{PT}$ Transition in Photonic Systems *Phys. Rev. Lett.* **111** 263901
[40] Yan Z Y 2013 Complex $\mathcal{PT}$-symmetric nonlinear Schrödinger equation and Burgers equation *Philos. Trans. R. Soc. Lond.* A **371** 20120059
[41] Yang J 2014 Symmetry breaking of solitons in one-dimensional parity-time symmetric optical potentials *Opt. Lett.* **39** 5547
[42] Xu W-X, Su S-J, Xu B, Guo Y-W, Xu S-L, Zhao Y and Hu Y-H 2020 Two dimensional spacial soliton in atomic gases with $\mathcal{PT}$-symmetry potential *Opt. Express* **28** 35297
[43] Shen Y, Wen Z, Yan Z and Hang C 2018 Effect of $\mathcal{PT}$ symmetry on nonlinear waves for three-wave interaction models in the quadratic nonlinear media *Chaos* **28** 043104
[44] Bagchi B and Quesne C 2010 An update on the $\mathcal{PT}$-symmetric complexified Scarf II potential, spectral singularities and some remarks on the rationally extended supersymmetric partners *J. Phys.* A **43** 305301
[45] Chen Y, Yan Z and Mihalache D 2020 Soliton formation and stability under the interplay between parity-time-symmetric generalized Scarf-II potentials and Kerr nonlinearity *Phys. Rev.* E **102** 012216
[46] Zhong M, Chen Y, Yan Z and Tian S-F 2022 Formation, stability, and adiabatic excitation of peakons and double-hump solitons in parity-time-symmetric Dirac-δ(x)-Scarf-II optical potentials *Phys. Rev.* E **105** 014204
[47] Zhong M, Yan Z and Tian S-F 2023 Stable matter-wave solitons, interactions, and excitations in the spinor F = 1 Bose-Einstein condensates with $\mathcal{PT}$-and non-$\mathcal{PT}$-symmetric potentials *Commun. Nonlinear Sci. Numer. Simulat.* **118** 107061
[48] Musslimani Z H, Makris K G, El-Ganainy R and Christodoulides D N 2008 Analytical solutions to a class of nonlinear Schrödinger equations with $\mathcal{PT}$-like potentials *J. Phys.* A **41** 244019
[49] Abdullaev F K, Kartashov Y V, Konotop V V and Zezyulin D A 2011 Solitons in $\mathcal{PT}$-symmetric nonlinear lattices *Phys. Rev.* A **83** 041805(R)
[50] Hu S, Ma X, Lu D, Yang Z, Zheng Y and Hu W 2011 Solitons supported by complex $\mathcal{PT}$-symmetric Gaussian potentials *Phys. Rev.* A **84** 043818
[51] Li X, Wang L and Yan Z 2023 Soliton formation and dynamics in the quintic nonlinear media with $\mathcal{PT}$-invariant harmonic-Gaussian potential *Phys. Lett.* A **459** 128607
[52] Zezyulin D A and Konotop V V 2012 Nonlinear modes in the harmonic $\mathcal{PT}$-symmetric potential *Phys. Rev.* A **85** 043840
[53] Dai C-Q, Wang X-G and Zhou G-Q 2014 Stable light-bullet solutions in the harmonic and parity-time-symmetric potentials *Phys. Rev.* A **89** 013834
[54] Znojil M 2020 Quantum phase transitions in nonhermitian harmonic oscillator *Sci. Rep.* **10** 1
[55] Chen Y, Yan Z and Mihalache D 2019 Stable flat-top solitons and peakons in the $\mathcal{PT}$-symmetric δ-signum potentials and nonlinear media *Chaos* **29** 083108
[56] Song J, Zhou Z, Weng W and Yan Z 2022 $\mathcal{PT}$-symmetric peakon solutions in self-focusing/defocusing power-law nonlinear media: Stability, interactions and adiabatic excitations *Physica* D **435** 133266
[57] Rosen N and Morse P M 1932 On the vibrations of polyatomic molecules *Phys. Rev.* **42** 210
[58] Znojil M 2000 Shape invariant potentials with $\mathcal{PT}$ symmetry *J. Phys.* A **33** L61
[59] Jia C-S, Zeng X-L and Sun L-T 2002 $\mathcal{PT}$ symmetry and shape invariance for a potential well with a barrier *Phys. Lett.* A **294** 185
[60] Jia C-S, Li S-C, Li Y and Sun L-T 2002 Pseudo-Hermitian potential models with $\mathcal{PT}$ symmetry *Phys. Lett.* A **300** 115
[61] Ishkhanyan H A and Krainov V P 2009 Resonance reflection by the one-dimensional Rosen-Morse potential well in the Gross-Pitaevskii problem *J. Exp. Theor. Phys.* **109** 585
[62] Lévai G 2012 Gradual spontaneous breakdown of $\mathcal{PT}$ symmetry in a solvable potential *J. Phys.* A **45** 444020
[63] Ahmed Z, Kumar S and Nathan J A 2022 $\mathcal{PT}$-symmetric potentials with imaginary asymptotic saturation *Pramana* **96** 144
[64] Midya B and Roychoudhury R 2013 Nonlinear localized modes in $\mathcal{PT}$-symmetric Rosen-Morse potential wells *Phys. Rev.* A **87** 045803
[65] Sun G-H and Dong S-H 2013 Quantum information entropies of the eigenstates for a symmetrically trigonometric Rosen-Morse potential *Phys. Scr.* **87** 045003

[66] Dai C-Q and Wang Y 2014 Higher-dimensional localized mode families in parity-time-symmetric potentials with competing nonlinearities *J. Opt. Soc. Am.* B **31** 2286

[67] Lévai G and Magyari E 2009 The $\mathcal{PT}$-symmetric Rosen-Morse II potential: effects of the asymptotically non-vanishing imaginary potential component *J. Phys.* A **42** 195302

[68] Chen Y, Yan Z and Malomed B A 2022 Higher-dimensional soliton generation, stability and excitations of the $\mathcal{PT}$-symmetric nonlinear Schrödinger equations *Physica* D **430** 133099

[69] Tiofack C G L, Ndzana F II, Mohamadou A and Kofane T C 2018 Spatial solitons and stability in the one-dimensional and the two-dimensional generalized nonlinear Schrödinger equation with fourth-order diffraction and parity-time-symmetric potentials *Phys. Rev.* E **97** 032204

[70] Tiofack C G L, Tchepemen N N, Mohamadou A and Kofane T C 2019 Stability of Gaussian-type soliton in the cubic-quintic nonlinear media with fourth-order diffraction and $\mathcal{PT}$-symmetric potentials *Nonlinear Dyn.* **98** 317

[71] Trefethen L N 2000 *Spectral Methods in Matlab* (Philadelphia: SIAM)

[72] Bender C M 2005 Introduction to $\mathcal{PT}$-symmetric quantum theory *Contemp. Phys.* **46** 277

[73] Bender C M, Hassanpour N, Hook D W, Klevansky S P, Sünderhauf C and Wen Z 2017 Behavior of eigenvalues in a region of broken $\mathcal{PT}$ symmetry *Phys. Rev.* A **95** 052113

[74] Yang J 2010 *Nonlinear Waves in Integrable and Nonintegrable Systems* (Philadelphia: SIAM)

[75] Yan Z, Wen Z and Konotop V V 2015 Solitons in a nonlinear Schrödinger equation with $\mathcal{PT}$-symmetric potentials and inhomogeneous nonlinearity: Stability and excitation of nonlinear modes *Phys. Rev.* A **92** 023821

[76] Zhang J R, Zhang J Q, Zheng Z L, Lin D and Shen Y J 2022 Dynamic behavior and stability analysis of nonlinear modes in the fourth-order generalized Ginzburg-Landau model with near $\mathcal{PT}$-symmetric potentials *Nonlinear Dyn.* **109** 1005